THE JOURNAL OF BIOLOGICAL CHEMISTRY VOL. 284, NO. 46, pp. 31798–31806, November 13, 2009

Deletion of a Genomic Segment Containing the Cardiac Troponin I Gene Knocks Down Expression of the Slow Troponin T Gene and Impairs Fatigue Tolerance of Diaphragm Muscle*

Received for publication, May 14, 2009, and in revised form, September 2, 2009 Published, JBC Papers in Press, September 21, 2009, DOI 10.1074/jbc.M109.020826

Han-Zhong Feng, Bin Wei, and Jian-Ping Jin[1]

From the Department of Physiology, Wayne State University School of Medicine, Detroit, Michigan 48201

The loss of slow skeletal muscle troponin T (TnT) results in a recessive nemaline myopathy in the Amish featured with lethal respiratory failure. The genes encoding slow TnT and cardiac troponin I (TnI) are closely linked. *Ex vivo* promoter analysis suggested that the 5′-enhancer region of the slow TnT gene overlaps with the structure of the upstream cardiac TnI gene. Using transgenic expression of exogenous cardiac TnI to rescue the postnatal lethality of a mouse line in which the entire cardiac TnI gene was deleted, we investigated the effect of enhancer deletion on slow TnT gene expression *in vivo* and functional consequences. The levels of slow TnT mRNA and protein were significantly reduced in the diaphragm muscle of adult double transgenic mice. The slow TnT-deficient (ssTnT-KD) diaphragm muscle exhibited atrophy and decreased ratios of slow *versus* fast isoforms of TnT, TnI, and myosin. Consistent with the changes toward more fast myofilament contents, ssTnT-KD diaphragm muscle required stimulation at higher frequency for optimal tetanic force production. The ssTnT-KD diaphragm muscle also exhibited significantly reduced fatigue tolerance, showing faster and more declines of force with slower and less recovery from fatigue as compared with the wild type controls. The natural switch to more slow fiber contents during aging was partially blunted in the ssTnT-KD skeletal muscle. The data demonstrated a critical role of slow TnT in diaphragm function and in the pathogenesis and pathophysiology of Amish nemaline myopathy.

Troponin T (TnT)[2] is a subunit of the troponin complex in striated muscles. Through interactions with troponin C, troponin I (TnI), and tropomyosin, TnT anchors the troponin complex to actin thin filament and plays a central role in the Ca^{2+} regulation of muscle contraction (1). Three TnT genes are present in the vertebrates: cardiac TnT, fast skeletal muscle TnT, and slow skeletal muscle TnT (ssTnT). They encode three muscle fiber type-specific TnT isoforms with differentiated expression and function (2).

A nonsense mutation at codon Glu^{180} in the ssTnT gene (*TNNT1*) causes a postnatal lethal form of inherited nemaline myopathy in the Amish (3). This mutation prematurely terminates the ssTnT polypeptide, and the C-terminally truncated ssTnT-(1–179) has a much decreased binding affinity for tropomyosin and fails to incorporate into the myofilaments (4). As a result, the truncated ssTnT protein was degraded and undetectable in the muscle of Amish nemaline myopathy patients, consistent with the recessive phenotype of the disease (5). Accordingly, the pathogenesis and muscle pathophysiology of Amish nemaline myopathy is due to the loss of slow TnT.

The genes encoding the muscle type-specific TnI and TnT isoforms are linked in tandem in three pairs in the vertebrate genome (2). The cardiac TnI (cTnI) (*TNNI3*) and ssTnT genes are very closely linked. Shown in *ex vivo* promoter analysis, the 5′ upstream enhancer region of the ssTnT gene overlaps with the structure of the cTnI gene (6). This structural integration of cTnI and ssTnT genes suggested that a previously developed mouse line in which the entire *Tnni3* gene was deleted through embryonic stem cell gene targeting (7) would have lost a large portion of the 5′-enhancer region of the *Tnnt1* gene (Fig. 1).

Although the *Tnni3*-deleted mouse line is a potentially useful model to study the phenotypes of ssTnT deficiency, a major hurdle is that the *Tnni3*-deleted mice die 16–18 days after birth from heart failure when the fetal expression of slow skeletal muscle TnI in the heart ceases (7). This postnatal lethality precluded functional examination on adult skeletal muscle for the phenotypes of ssTnT deficiency. However, adult skeletal muscle is necessary for investigating the pathophysiology of Amish nemaline myopathy because the fetal and neonatal expression of cardiac TnT in skeletal muscles (8) may functionally compensate for the loss of ssTnT in (5).

We previously developed two transgenic mouse lines overexpressing an N-terminal truncated cTnI (cTnI-ND) driven by an α-myosin heavy chain (MHC) promoter (9). cTnI-ND was originally found as a product of restricted proteolysis in cardiac adaptation to simulated microgravity, which selectively removes the cTnI-specific N-terminal extension and leaves the conserved structure intact (10). cTnI-ND transgenic mice exhibit normal base-line life activity with an increased relaxation of the cardiac muscle (9). Using this postnatally up-regulated (11) transgene allele encoding a non-destructive exogenous TnI, we successfully

* This work was supported, in whole or in part, by National Institutes of Health Grants AR-048816 and HL-078773 (to J.-P. J.).

[1] To whom correspondence should be addressed: Dept. of Physiology, Wayne State University School of Medicine, 540 E. Canfield, Detroit, MI 48201. Tel.: 313-577-1520; Fax: 313-577-5494; E-mail: jjin@med.wayne.edu.

[2] The abbreviations used are: TnT, troponin T; TnI, troponin I; cTnI, cardiac TnI; cTnI-KO, cTnI knockout; cTnI-ND, N-terminal truncated cTnI; mAb, monoclonal antibody; MHC, myosin heavy chain; PBS, phosphate-buffered saline; ssTnT, slow skeletal muscle TnT; ssTnT-KD, ssTnT knockdown.

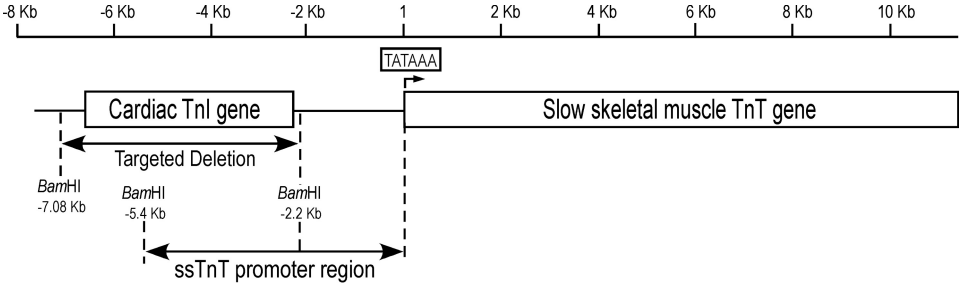

FIGURE 1. **Targeted deletion of cTnI gene in the mouse genome removes the 5′ portion of the ssTnT gene promoter-enhancer region.** The cTnI gene and ssTnT gene are very closely linked in the mouse genome with the 5′ portion of the ssTnT gene promoter-enhancer region integrated in the structure of the cTnI gene (6). The targeted deletion of the entire cTnI gene in a cTnI knock-out mouse line (7) had concurrently removed a segment containing 5′-enhancer(s) of the ssTnT gene promoter, which would reduce transcriptional activity as indicated by significantly decreased transcriptional activity of the −2.2 kb promoter construct *versus* the −5.4 kb control in previous *ex vivo* experiments (6).

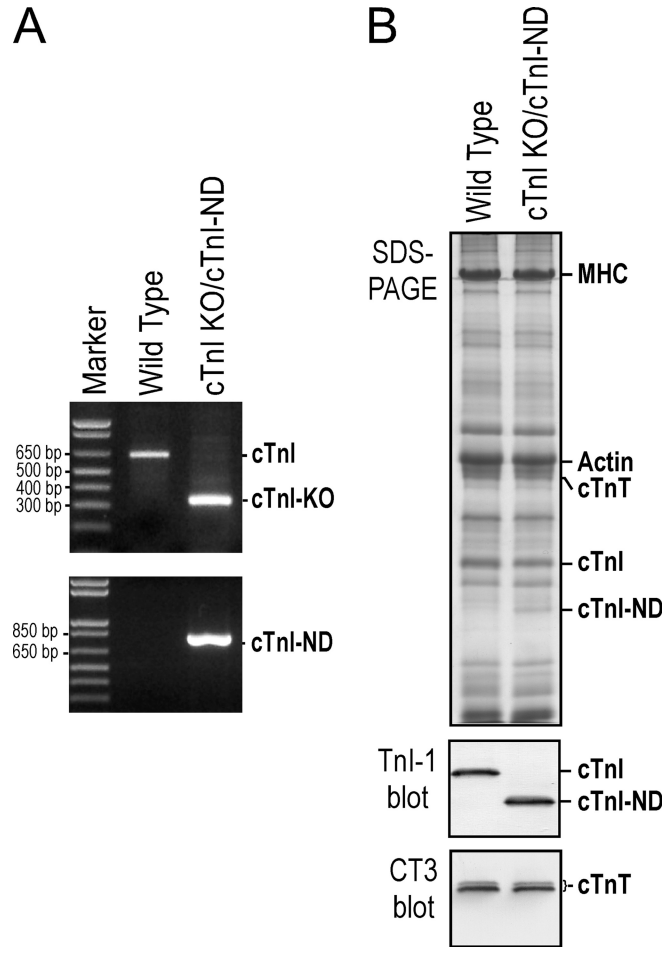

FIGURE 2. **Rescue of cTnI gene deletion mice by transgenic expression of cTnI-ND.** *A*, the two agarose gels demonstrated the PCR genotyping of double transgenic mice using two pairs of specific primers recognizing wild type and *Tnni3* deletion alleles, respectively (7), to identify homozygote of cTnI gene deletion (*top*) and the presence of α-MHC promoter-directed transgene encoding cTnI-ND (*bottom*). *B*, the SDS-gel and Western blot using mAb TnI-1 showed that the cardiac muscle of adult double transgenic mice expressed cTnI-ND in the absence of endogenous cTnI, demonstrating a successful rescue of the postnatal lethality of cTnI-KO mice. The mAb CT3 Western blot showed normal expression of cardiac TnT (*cTnT*) in the double transgenic mouse cardiac muscle.

rescued the postnatal lethality of the *Tnni3* gene-deleted mice (12) to produce adult skeletal muscle for investigating the functional effects of ssTnT deficiency.

Amish nemaline myopathy is a rapidly progressive disorder, with affected children dying primarily from respiratory insufficiency due to weakness of the respiratory muscle, usually in the second year of life (3). These clinical features suggest a critical role of ssTnT in diaphragm function. Therefore, we examined in the present study the phenotypes of diaphragm muscle of adult double transgenic mice. The results revealed significantly decreased expression of ssTnT mRNA and protein. The ssTnT deficiency produced atrophy and a change toward more fast fibers in the diaphragm muscle. The slow TnT-deficient diaphragm muscle had significantly decreased tolerance to fatigue, demonstrating a critical role of ssTnT in respiratory function.

MATERIALS AND METHODS

Tnni3-deleted/cTnI-ND Double Transgenic Mice—As described recently (12), we crossed transgenic mouse line cTnI-ND#7 (9) with heterozygotes of *Tnni3*-deleted mice (7), provided by Dr. Xupei Huang (Florida Atlantic University). The genotyping of the double transgenic offspring was performed on genome DNA isolated from tail biopsies using PCR, and the compensation for the loss of endogenous cTnI by cTnI-ND in cardiac muscle was confirmed by Western blotting as described (7, 9) (Fig. 2).

The mice were maintained on a 12-h light/12-h dark cycle (6:00 a.m./6:00 p.m.) and standard pellet diet. Except for aging studies, mice at age 3–5 months of both sexes were used for phenotype characterization. Immediately after euthanasia with pentobarbital (intraperitoneally, 100 mg/kg), diaphragm muscle strips were dissected from the 9 o'clock and 4 o'clock sectors with the dorsal side as 12 and 1 o'clock positions (13) for use in the experiments to avoid the difference between different portions of the diaphragm. All animal procedures were approved by the Institutional Animal Care and Use Committee.

Quantitative PCR—Total RNA was extracted from mouse diaphragm muscle samples using the TRIzol reagent (Invitrogen). Integrity of the isolated RNA was verified using agarose gel electrophoresis. One μg of each RNA was reverse transcribed using an anchored oligo(dT) primer (TV20) at 42 °C for 2 h. Quantitative PCR was carried out with Power SYBR Green PCR master mix (Applied Biosystems) to determine the level of ssTnT cDNA relative to the level of glyceraldehyde-3-phosphate dehydrogenase, using an Applied Biosystems 7300 real time PCR system (Applied Biosystems, Foster City, CA). The PCR primers (Fig. 3*A*) were designed to target the common sequence for all three alternatively spliced isoforms of ssTnT mRNA (14) without cross-reaction with fast skeletal muscle TnT cDNA (Fig. 3*B*). The quantitative PCR was carried out in a 20-μl volume with a 10-min preheating at 95 °C followed by 40 cycles of 15 s at 95 °C and 60 s at 60 °C. Melting curve analysis was performed at the end to verify that there was no significant

formation of primer dimmers under the PCR conditions. Diaphragm samples from three wild type and three double transgenic mice were examined, each with triplicate reactions. The results were analyzed using the $2^{-\Delta\Delta Ct}$ method as per the Applied Biosystems user's instructions.

SDS-PAGE and Western Blot—Endogenous cTnI and exogenous cTnI-ND in the heart and TnT and TnI isoforms in the diaphragm muscle were examined by SDS-PAGE and Western blotting. Total protein was extracted from freshly isolated muscle tissue by homogenization in SDS-PAGE sample buffer containing 2% SDS to inactivate tissue proteases. The samples were heated at 80 °C for 5 min, centrifuged at top speed in a microcentrifuge for 5 min to remove insoluble materials, and stored at −80 °C until use.

The protein samples were resolved on 14% Laemmli gels with an acrylamide/bisacrylamide ratio of 180:1. The resulting gels were stained with Coomassie Blue R250 or electrically transferred to nitrocellulose membrane using a semidry transfer apparatus (Bio-Rad). After blocking in Tris-buffered saline containing 1% bovine serum albumin, the membranes were probed using anti-TnI monoclonal antibody (mAb) TnI-1, anti-slow and cardiac TnT mAb CT3 (14), or anti-fast TnT mAb T12 (a gift from Prof. Jim Lin, University of Iowa) (15). The first antibody reactions were in Tris-buffered saline containing 0.1% bovine serum albumin at 4 °C overnight. The subsequent washes, alkaline phosphatase-labeled anti-mouse IgG second antibody (Santa Cruz Biotechnology, Inc., Santa Cruz, CA) incubation, and 5-bromo-4-chloro-3-indolylphosphate/nitro blue tetrazolium substrate reaction were carried out as described previously (16). The relative amounts of TnT and TnI isoforms were quantified by two-dimensional densitometry of the blots.

Myosin heavy chain isoforms were examined as described previously (17). The muscle protein samples were resolved on 8% SDS-polyacrylamide gel containing 30% glycerol run in an icebox overnight. The gels were stained with Coomassie Blue R250, and the relative amounts of MHC isoforms were quantified by two-dimensional densitometry.

Hematoxylin-Eosin Staining of Paraffin Sections—After euthanasia of the mice, diaphragm tissue was rapidly excised and fixed in 3.7% formaldehyde in phosphate-buffered saline (PBS). The diaphragm samples were embedded in paraffin with precise orientation and thin cross sections were cut and processed with hematoxylin-eosin staining at a service facility for light microscopic examinations.

Immunohistochemistry—Mouse diaphragm muscle samples were rapidly frozen in a small drop of O.C.T. compound in isopentane at −159 °C and then embedded in O.C.T. for thin frozen cross sectioning. The sections were fixed in 75% acetone, 25% ethanol for 5 min.

After blocking in PBS containing 0.05% Tween 20 (PBS-T) and 1% bovine serum albumin for 30 min, the sections were incubated with 1% H_2O_2 in PBS for 10 min to inactivate endogenous peroxidases. The sections were then washed with PBS-T three times and incubated with anti-MHC-I mAb FA2 or SP2/0 myeloma culture supernatant at 4 °C overnight. After washes with PBS-T to remove unbound mAb, the sections were incubated with horseradish peroxidase-labeled anti-mouse secondary antibody at room temperature for 1 h, washed again, and developed in 3,3′-diaminobenzidine-H_2O_2 substrate solution in the dark for 30–60 s. The substrate reaction was stopped by washes in 20 mM Tris-HCl, pH 7.6, for six changes.

After they were counterstained with hematoxylin for 5 min and water washes, the sections were immersed in a drop of 50% glycerol in PBS and mounted with Cytoseal. The slides were examined under a Zeiss Observer microscope and photographed. FA2-positive (type 1) fibers were counted per unit of cross-sectional area for comparisons.

Contractility Measurements—Mouse diaphragm muscle was isolated immediately after euthanasia as above. Immersed in Krebs solution (118 mM NaCl, 25 mM $NaHCO_3$, 4.7 mM KCl, 1.2 mM KH_2PO_4, 2.25 mM $MgSO_4$, 2.25 mM $CaCl_2$, and 11 mM D-glucose, pH 7.4) continuously bubbled with 95% O_2 plus 5% CO_2 at room temperature, 2-mm-wide diaphragm muscle strips were dissected with a piece of central tendon at one end and a piece of the rib cage tissue at the other end. The rib cage end of the muscle strip was tied to a triangle-shaped stainless steel hook with a #5-0 suture. The muscle strip was then mounted to the bottom pole of a vertical bath (Radnoti) containing Krebs bubbled with 95% O_2 plus 5% CO_2 at 25 °C, and the tendon end was tied to another stainless steel hook for connection to a motorized force transducer (model 300B-LR, Aurora Scientific, Inc.). Isometric twitch contractions were stimulated by 20-V field electrical pulses of 0.2-ms duration using an Aurora 701B stimulator. Force of the muscle strip was measured, and length was controlled through the 300B-LR transducer, and data were collected via a digital controller A/D interface (model 604C, Aurora Scientific Inc.).

The mounted muscle strip was adjusted to an optimal length for the production of maximal twitch force during 30 min of equilibration. 500-ms tetanic contractions were then stimulated every 1 min with 100-Hz 20-V field electrical pulses of 0.2-ms duration for 20 min. The force-frequency relationship was determined from isometric tetanic contractions stimulated with electrical pulses at various frequencies (60–240 Hz).

High Frequency and Intermittent Fatigue Protocols—The diaphragm muscle was examined for high frequency fatigability in which tetanic contractions were stimulated with 20-V field electrical pulses of 0.2-ms duration at the optimal frequency for 30 s, followed by stimulations with electrical pulses of 2.0-ms duration for 5 s to bypass the membrane electrical fatigability (18). The effect of bypassing membrane electrical fatigability was verified by pulse stimulations of 2.0-ms duration for 30 s followed by 3.0-ms pulses for 5 s. One minute after the high frequency fatigue contractions, 500-ms tetanic contractions were stimulated every 1 min with 20-V field electrical pulses of 0.2-ms duration at the optimal frequency for 20 min to monitor the recovery.

Fatigability of the diaphragm muscle was also examined with intermittent tetanic contractions in which 330 ms of tetanic contraction was evoked every 2 s (a duty cycle of 16.5%), as described previously (19, 20) with 20-V field electrical pulses of 0.2-ms duration at the optimal frequency for 7 min. One minute after the intermittent fatigue contractions, 20 min of recovery was monitored as above.

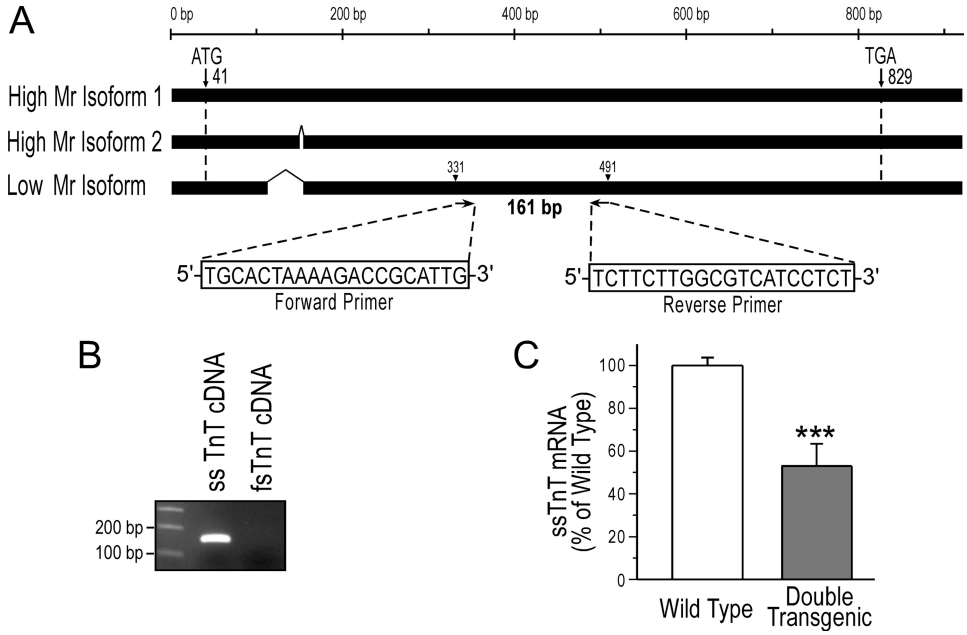

FIGURE 3. **Decreased expression of ssTnT mRNA in diaphragm muscle of double transgenic mice.** *A*, for quantitative PCR, a pair of oligonucleotide primers were designed for a region identical in the three alternatively spliced isoforms of ssTnT mRNA. *B*, the agarose gel verified the specificity of the primers in PCR on cloned ssTnT and fast skeletal muscle TnT (*fsTnT*) cDNA templates. *C*, quantifications using real-time PCR detected a significantly decreased level of ssTnT mRNA in the diaphragm muscle of cTnI-KO/cTnI-ND double transgenic mice in comparison with the wild type control. Values are shown as mean ± S.E., $n = 3$ mice in each group. ***, $p < 0.001$ in two-tailed Student's *t* test.

All muscle strips used for the functional studies were recovered at the end of the experiment and examined by SDS-PAGE and Western blot to verify ssTnT and other myofilament protein contents.

Data Analysis—Two-dimensional densitometry was used to quantify the SDS-gel and Western blots scanned at 600 dots/inch using Image J software. Using Image J software, the average thickness of the diaphragm was measured in 600-μm intervals along the tissue sections, and the cross-sectional area of muscle fibers was calculated. The data are shown as mean ± S.E., and statistical significance was determined using two-tailed unpaired Student's *t* test. Difference was considered significant when p was <0.05.

RESULTS

Decreased ssTnT mRNA in Diaphragm Muscle of Adult Double Transgenic Mice—Quantitative PCR with primers recognizing all three alternatively spliced isoforms of ssTnT but not fast TnT mRNA showed significantly decreased expression of ssTnT mRNA in diaphragm muscle of adult cTnI-KO/cTnI-ND double transgenic mice as compared with that in wild type mouse diaphragm muscles (Fig. 3). Therefore, the deletion of the 5′ portion of the ssTnT gene enhancer-promoter region integrated in the cTnI gene resulted in a knockdown effect on the transcription of the ssTnT gene *in vivo*.

Decreased ssTnT Protein in Diaphragm Muscle of Young Adult Double Transgenic Mice—Western blots using mAb CT3 detected decreased ssTnT protein (down by ~39%) in diaphragm muscle of cTnI-KO/cTnI-ND double transgenic mice as compared with that in wild type control (Fig. 4*A*). Together with the decreased ssTnT mRNA, the results demonstrated that the double transgenic mice provide a model of ssTnT deficiency for investigating the function of ssTnT in adult diaphragm muscle. The double transgenic mice are referred as ssTnT-KD in the following phenotype characterizations.

Corresponding to the decreased ssTnT, Western blots using mAb T12 showed that fast TnT in the ssTnT-KD diaphragm muscle was increased by ~15% as compared with the level in wild type mouse diaphragm muscle (Fig. 4*A*).

Decreases in the Slow Isoforms of TnI and MHC in ssTnT-KD Diaphragm—In 3–5-month-old young adult ssTnT-KD mice, Western blots with mAb TnI-1 recognizing all TnI isoforms showed that slow TnI was significantly decreased (down by ~25%) and fast TnI increased as compared with the wild type controls (Fig. 4*A*).

Glycerol SDS-PAGE showed decreases of MHC-I in the adult ssTnT-KD diaphragm muscle (~8.6% of total MHC *versus* ~13.8% in wild type control diaphragm) (Fig. 4*B*). Trends of reduction of MHC-IIa and potentially compensatory increases in MHC-IIx and MHC-IIb were also observed (Fig. 4*B*).

Decreased Number of Type 1 Slow Fibers and Atrophy in ssTnT-KD Diaphragm Muscle—Type 1 slow fibers in mouse diaphragm muscle were identified by staining frozen thin cross-sections using anti-MHC-I mAb FA2. The results detected a significantly decreased number of type 1 fibers in 3–5-month-old ssTnT-KD mouse diaphragm muscle (~52% of the wild type control normalized to unit area) (Fig. 5*A*). Correspondingly, FA2-negative type 2 fibers were increased by ~28% in the ssTnT-KD diaphragm muscle as compared with that in wild type control. These changes resulted in a significant decrease in the ratio of slow/fast fiber in the young adult ssTnT-KD diaphragm muscle (~0.2) *versus* that in wild type control (~0.5) (Fig. 5*A*).

Microscopic measurement of hematoxylin-eosin-stained paraffin cross-sections showed that the young adult ssTnT-KD mouse diaphragm was thinner than that of wild type control (~0.33 *versus* ~0.37 mm; Fig. 5*B*), indicating muscle atrophy. Comparing the cross-sectional area of type 1 and type 2 fibers, we further observed significant atrophy of type 1 fibers (~43% of the wild type control; Fig. 5*B*). Interestingly, the cross-sectional area of type 2 fibers was also decreased in ssTnT-KD diaphragm muscle although less severely than that of the type 1 fibers (~88% of the wild type controls; Fig. 5*B*).

Higher Stimulating Frequency Required for the Production of Maximum Tetanic Force in ssTnT-KD Diaphragm Muscle—We studied the force-frequency relationships in tetanic contraction of wild type and ssTnT-KD mouse diaphragm muscle strips. A right-

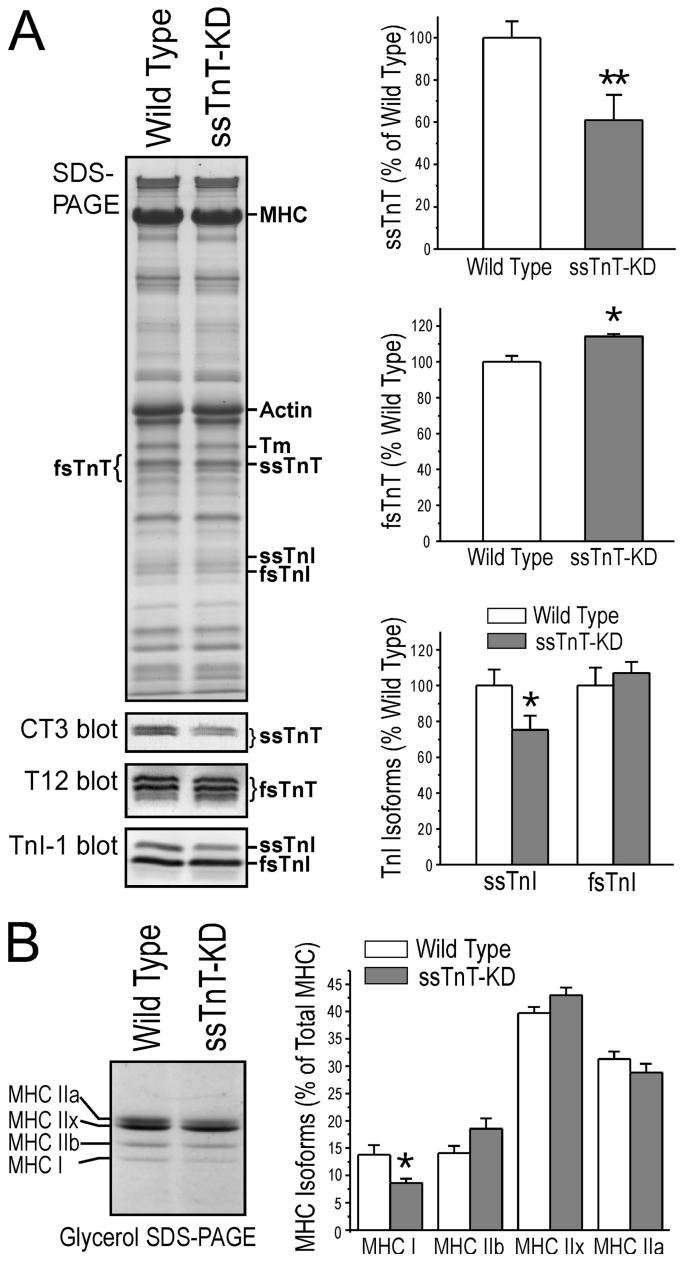

FIGURE 4. **Decreased ssTnT and the slow isoforms of TnI and MHC in diaphragm muscle of young adult ssTnT-KD mice.** *A*, SDS-gel and mAb CT3 Western blot densitometry detected significantly lower levels of ssTnT protein in diaphragm muscle of the ssTnT-KD mice as compared with the wild type controls (down by 39.1 ± 9.6% normalized to the level of actin in accompanying gels). Correspondingly, mAb T12 Western blot and densitometry analysis detected higher levels of fast skeletal muscle TnT (*fsTnT*) in the ssTnT-KD diaphragm muscle than the wild type controls (up by 14.99% normalized to the level of actin in accompanying gels). Densitometry analysis of mAb TnI-1 Western blot normalized to the amount of total TnI found decreased the slow *versus* fast isoform ratio of TnI in the ssTnT-KD diaphragm muscle as compared with the wild type controls. *B*, glycerol-SDS-gel and densitometry analysis normalized to total MHC showed a decreased level of MHC-I in ssTnT-KD diaphragm muscle (8.62% of total MHC *versus* 13.83% in wild type control). *, $p < 0.05$ by two-tailed Student's *t* test.

ward shift of the force-frequency relationship curve was found in young adult ssTnT-KD diaphragm muscle as compared with wild type control (Fig. 6). The optimal frequencies at which the maximal tetanic force was generated in wild type and ssTnT-KD diaphragm muscles were around 120 and 140 Hz, respectively. This shift indicates an increased dependence of the ssTnT-KD diaphragm muscle on stimulating frequency in tetanic force production, consistent with a faster muscle phenotype.

Whereas most of the twitch contraction parameters did not show significant difference between the ssTnT-KD and wild type mouse diaphragm muscle strips, the shorter time of tension development (TPT and TP_{50}) of the ssTnT-KD diaphragm muscle was also consistent with a faster muscle phenotype (Table 1). Although ssTnT-KD diaphragm muscle produced lower tetanic force at the stimulating frequency optimal for wild type diaphragm muscle (Fig. 6), tetanic contractile force generated at its own optimal frequency of stimulation was not significantly different from that of the wild type control (Table 1).

Unchanged Electrical Fatigability and Increased Myofilament Fatigability of ssTnT-KD Diaphragm Muscle—Because electrical pulses of short duration induce skeletal muscle contraction dependent on the propagation of action potential along the plasma membrane, we used a high frequency fatigue protocol to study the membrane electrical fatigability of the mouse diaphragm muscle strips. The results in Fig. 7*A* showed that wild type and ssTnT-KD young adult mouse diaphragm muscles had no difference in membrane fatigability during a 30-s tetanic contraction stimulated with field electrical pulse of 0.2-ms duration at the optimal frequencies. Switching to electrical pulse stimulations of 2-ms duration at the end of the protocol significantly increased the tetanic force production of both wild type and ssTnT-KD groups to the same extent (Fig. 7*A*). The similar increases in force production upon bypassing membrane fatigability using brief wider electrical pulse stimulations (18) indicated similar extents of myofilament fatigability in the wild type and ssTnT-KD mouse diaphragm muscle strips when the contractile apparatus was protected by membrane fatigability. Consistently, both wild type and ssTnT-KD diaphragm muscle strips completely recovered from the electrical fatigue treatment (data not shown).

In a modified high frequency fatigue protocol using pulse stimuli of 2.0-ms duration followed by a switch to 3.0-ms pulse duration, we further investigated the fatigability of mouse diaphragm muscle bypassing the membrane electrical dependence. The results in Fig. 7*B* revealed a significant difference between ssTnT-KD diaphragm muscle strips and the wild type controls. The faster and more extensive decreases in tetanic force of ssTnT-KD diaphragm muscle indicated increased myofilament fatigability in comparison with the wild type control. When the duration of electrical pulses was switched from 2.0 to 3.0 ms, there were small increases in tetanic force in both ssTnT-KD and wild type groups, suggesting that the calcium mobilization capacity (18) was not exhausted in the diaphragm muscle fibers when stimulated by 20-V field pulses of 2.0-ms duration.

Increased Fatigability and Decreased Recovery of ssTnT-KD Diaphragm Muscle in Intermittent Tetanic Contractions—The increased myofilament fatigability in ssTnT-KD diaphragm muscle was further examined using a 7-min intermittent fatigue protocol. The results in Fig. 8*A* showed that 210 cycles of intermittent tetanic contraction at 16.5% duty cycle (330-ms trains) stimulated with 0.2-ms electrical pulses at optimal frequency exhibited force decreases to ~40.5% of the prefatigue level in ssTnT-KD diaphragm muscle as compared with

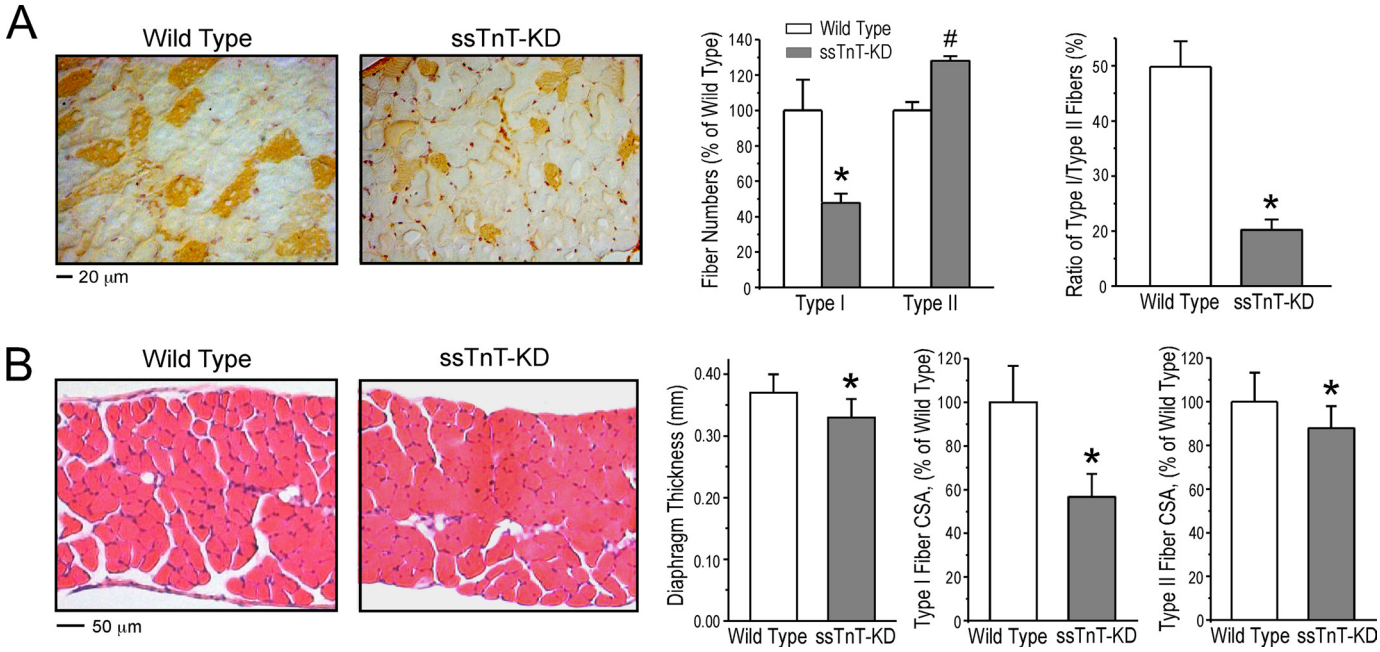

FIGURE 5. **Atrophy and type 1 fiber reduction of ssTnT-KD diaphragm muscle.** *A*, immunostaining of frozen sections using anti-MHC-I mAb FA2 showed 52.2 ± 4.9% decrease in type 1 fibers and 28.0 ± 5.2% increase of type 2 fibers in ssTnT-KD diaphragm muscle as compared with the wild type control. Accordingly, the ratio of type 1/type 2 fibers was much lower in ssTnT-KD mouse diaphragm muscle (20.2 ± 1.7%) than that in wild type control muscles (49.8 ± 4.7%). *B*, hematoxylin-eosin-stained cross-sections showed that the thickness of adult ssTnT-KD mouse diaphragm was smaller (0.33 ± 0.03 mm) than that of wild type controls (0.37 ± 0.03 mm), indicating muscle atrophy. Morphological analysis further found that the cross-sectional area (*CSA*) of type 1 fibers was significantly decreased by 43.2 ± 6.2% in ssTnT-KD diaphragm as compared with the wild type control. The cross-sectional area of type 2 fibers in ssTnT-KD diaphragm was also decreased, although by a lesser extent (12.1 ± 3.2%), as compared with the wild type control. *, $p < 0.05$ by two-tailed Student's *t* test.

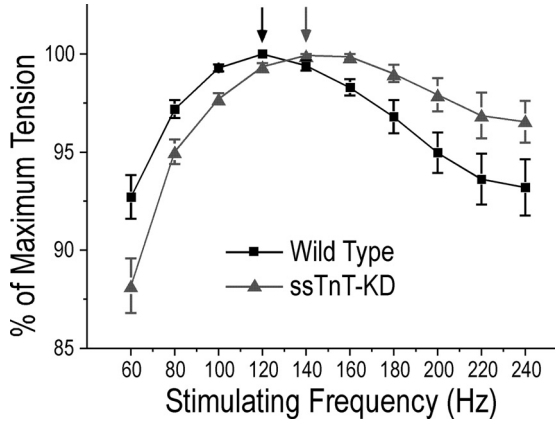

FIGURE 6. **Shift of force-frequency relationship in ssTnT-KD diaphragm muscle.** Tetanic force production was examined with electrical pulse stimulations of 0.2-ms duration at 60–240 Hz in 20-Hz increments. The results showed that ssTnT-KD diaphragm muscle had optimal frequency for maximum force at 140 Hz, increased from 120 Hz for the wild type mouse diaphragm muscle, consistent with increased fast fiber content. *, $p < 0.05$ by two-tailed Student's *t* test, $n = 3$ mice in each group.

TABLE 1

Parameters of twitch and tetanic contractions

Data are presented as mean ± S.E. $n = 10$ mice for wild type and $n = 11$ mice for ssTnT-KD groups. mN, millinewtons; dT/dt, develop tension; TP_{50}, time to reach 50% peak tension; TPT, time to reach peak tension; TR_{75}, time to reach 75% relaxation.

	Wild type	ssTnT-KD
Developed twitch tension (mN/mm^2)	46.05 ± 3.23	40.23 ± 4.84
+dT/dt (mN/s)	1683.6 ± 20.6	1458.3 ± 16.4
−dT/dt (mN/s)	−851.8 ± 82.0	−750.8 ± 66.9
TP_{50} (ms)	10.73 ± 0.19	10.08 ± 0.23[a]
TPT (ms)	28.91 ± 0.79	25.50 ± 0.68[b]
TR_{75} (ms)	32.25 ± 2.84	30.75 ± 2.06
Optimal tetanic tension (mN/mm^2)	187.82 ± 12.16	209.37 ± 13.32

[a] $p < 0.05$ in two-tailed Student's *t* test.
[b] $p < 0.01$ in two-tailed Student's *t* test.

~54.4% in wild type control muscle strips. The 20-min recovery from fatigue treatment showed that tetanic force went back to ~98.5% of the prefatigue level in wild type diaphragm muscle but only to ~91.6% in the ssTnT-KD group (Fig. 8*B*). The data indicated that the slow TnT deficiency resulted in significantly increased myofilament fatigability in the young adult diaphragm muscle of ssTnT-KD mice.

Effects of ssTnT-KD on Contractility and Myofilament Protein Isoform Contents of Aging Diaphragm—We further examined diaphragm muscle from 13–20-month-old mice for contractility and myofilament protein isoform expression to investigate the effect of ssTnT-KD. The results in Fig. 9*A* showed that aging wild type and ssTnT-KD diaphragm muscles both switched toward slower fiber type, whereas the ssTnT-KD group remained faster than the wild type control, consistent with the previous observation that aging skeletal muscles undergo a shift to more aerobic-oxidative metabolism in a slower twitching fiber population (21, 22).

Slow TnT and slow TnI remained low in aging ssTnT-KD diaphragm muscle (Fig. 9*B*). Consistent with the shift toward slower muscle type, the slow/fast isoform ratio of TnI increased in aging wild type diaphragm muscle but was insignificant in ssTnT-KD diaphragm (Fig. 9*B*). The level of MHC-IIa increased in aging diaphragm muscles of wild type mice with a lesser degree in ssTnT-KD group (Fig. 9*B*). MHC-IIx decreased during aging in both groups (Fig. 9*B*).

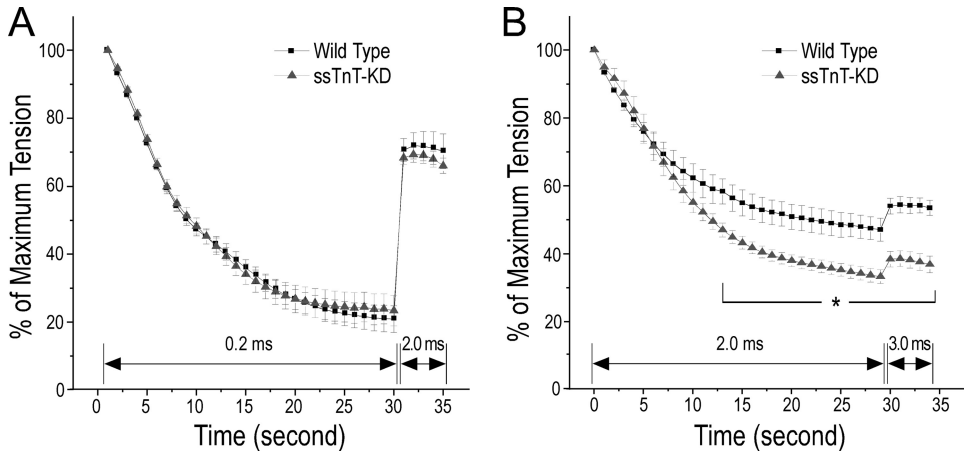

FIGURE 7. **High frequency fatigue analysis.** *A*, a high frequency fatigue protocol was tested on diaphragm muscle strips with field electrical stimuli of 0.2-ms duration for 30 s followed by 2.0-ms stimuli for 5 s. The results showed no difference in electrical fatigability between the ssTnT-KD and wild type diaphragm muscles. Switch of the electrical pulses from 0.2-ms duration to 2.0-ms duration generated similar partial recovery of the contractile force in both groups, suggesting similar protection of the muscle by electrical fatigue. *B*, high frequency fatigue analysis was modified to bypass the membrane dependence using electrical stimuli of 2.0-ms duration for 30 s followed by stimuli of 3.0-ms duration for 5 s. The results showed significantly higher myofilament fatigability of ssTnT-KD diaphragm muscle as compared with the wild type control. *, $p < 0.05$ by two-tailed Student's *t* test, $n = 6$ mice in each group.

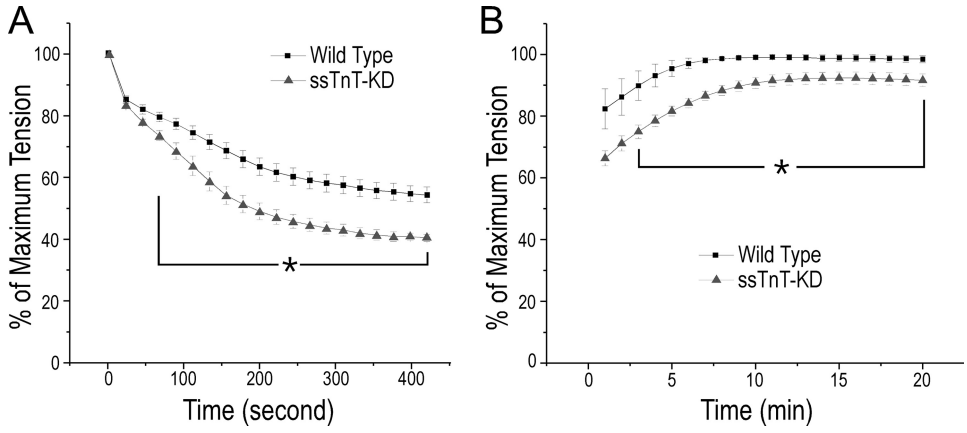

FIGURE 8. **Intermittent fatigability analysis.** *A*, an intermittent fatigue protocol was applied to examine wild type and ssTnT-KD mouse diaphragm muscle strips. Tetanic contractions stimulated at optimum frequency with 330-ms/2-s trains for 7 min demonstrated force declines to 54.4 ± 2.6% in wild type and to 40.5 ± 1.1% in ssTnT-KD diaphragm muscle strips. *B*, during a 20-min recovery, the force of wild type diaphragm muscle returned to 98.5 ± 1.2% of the prefatigue level, whereas that of ssTnT-KD diaphragm muscle returned to 91.6 ± 2.0% of the prefatigue level. *, $p < 0.05$ by two-tailed Student's *t* test, $n = 6$ mice in each group.

In contrast to the significant decrease in MHC-IIb in aging wild type mouse diaphragm muscle, the level of MHC-IIb increased in ssTnT-KD mouse diaphragm during aging (Fig. 9*B*). Although determination of its functional significance requires follow up studies, this finding indicated that the decrease in slow TnT induced adaptive gene regulations for the expression of other myofilament proteins with differentiated effects in young and aging skeletal muscles.

DISCUSSION

Troponin T abnormalities have been found in causing diseases in both cardiac and skeletal muscles (23). We and others have extensively studied the biochemical mechanisms for the structure-function relationship of TnT isoforms (2, 24). It has been shown that slow TnT has differentiated binding affinity for TnI and tropomyosin and confers higher Ca^{2+} sensitivity in comparison with that of fast TnT (5, 13). The present study demonstrated the importance of slow TnT in the function of skeletal muscle. Our findings provide some new insights into the following aspects.

The Structural Linkage of cTnI and ssTnT Genes—Cardiac TnI and ssTnT genes are very closely linked in the vertebrate genome. We previously detected in *ex vivo* promoter analysis that the kb −2.2 to −5.4 upstream region of the ssTnT gene, which overlaps with the 3′ region of the cTnI gene, contained major enhancer activity required for high level transcription of the ssTnT gene (6). The present study further demonstrated that deletion of the cTnI gene between the two BamHI sites (Fig. 1*A*) (7), equivalent to the −2.2 kb deletion of the upstream region of ssTnT gene tested *ex vivo*, had a destructive effect *in vivo* on the promoter activity of the ssTnT gene. Because a single copy of a functional ssTnT gene was sufficient in sustaining muscle function in heterozygote careers of Amish nemaline myopathy (5), the decreased level of ssTnT in the diaphragm muscle of ssTnT-KD mice indicated a more than 50% decrease of ssTnT gene promoter activity due to deletion of the −2.2 kb upstream genomic enhancer segment.

Although the ssTnT gene is identified to be the newest member evolved among the three muscle type TnT isoform genes (25), its function is indispensable, and the loss of ssTnT causes a lethal phenotype in Amish nemaline myopathy (5). This functional importance might have been responsible for the ssTnT gene remaining closely linked to the upstream cTnI gene during evolution, because a destruction of either the 3′-coding exons of the cTnI gene or the 5′-enhancer region of the ssTnT gene would cause infantile lethality (5, 7).

The Effects of ssTnT Deficiency on Myofilament Protein Isoforms and Atrophy of Diaphragm Muscle—The primary ssTnT deficiency resulted a series of secondary changes in the diaphragm muscle of young adult ssTnT-KD mice. In addition to an increased ratio of fast TnT, ssTnT-KD diaphragm muscle showed decreased slow TnI and a trend of increase in fast TnI. MHC-I was decreased together with trends of increases in MHC-IIx and MHC-IIb. Therefore, the primary deficiency of ssTnT resulted in reductions of the slow isoforms of both thin and thick filament proteins. The decreased slow/fast isoform

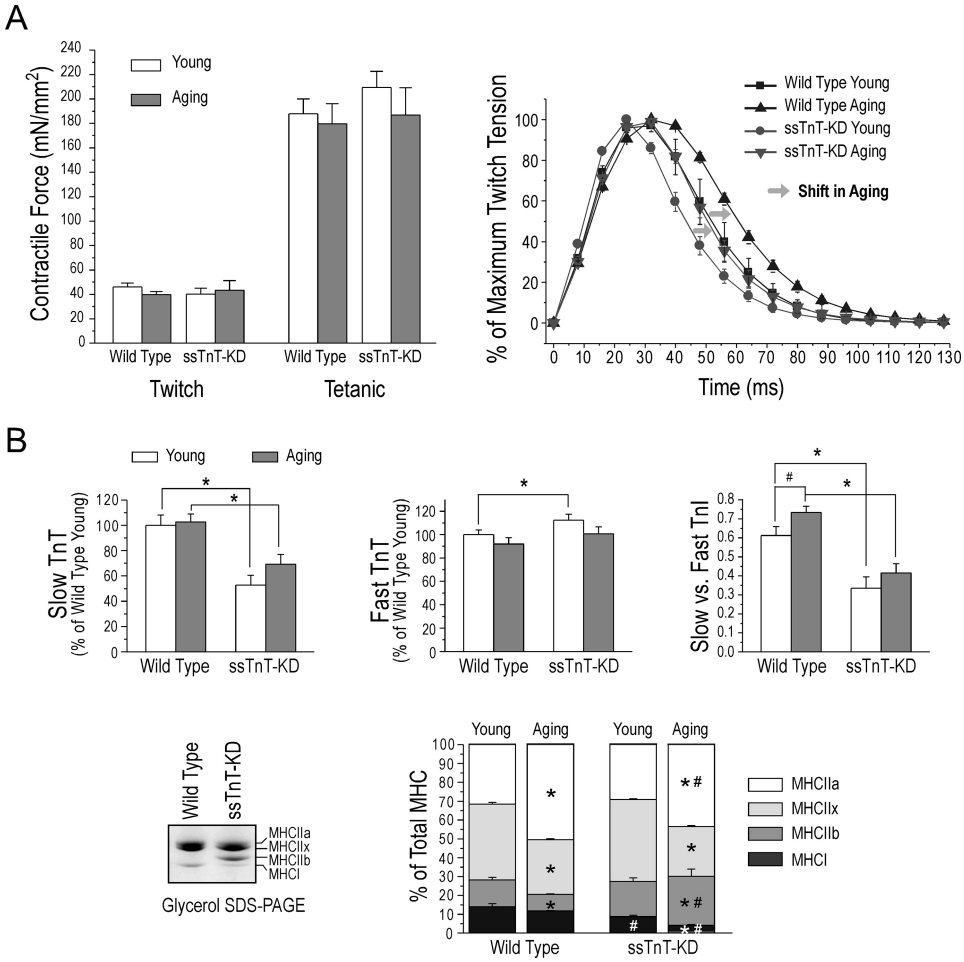

FIGURE 9. **Effects of ssTnT-KD in aging diaphragm muscle.** *A* (*left*), twitch and tetanic force measurements found no significant difference between young and aging diaphragm muscles from wild type and ssTnT-KD mice. *Right*, normalized twitch contraction curves revealed that wild type and ssTnT-KD mouse diaphragm muscles both shifted toward slower fiber type in aging, whereas the ssTnT-KD group remained faster than the wild type control. *B* (*top*), densitometry analysis of CT3, T12, and TnI-1 mAb Western blots showed that slow TnT remained low in aging diaphragm muscle of ssTnT-KD mice along with the trend of higher fast TnT contents and decreased slow *versus* fast isoform ratio of TnI as compared with the wild type controls. *Bottom*, glycerol-SDS-gel and densitometry analysis showed that MHC-I went down in aging diaphragm muscle with much more severity in the ssTnT-KD group than in the wild type control. MHC-IIa was increased during aging to a lesser degree in ssTnT-KD than that in wild type diaphragms. There was a trend of decrease in MHC-IIx in both wild type and ssTnT-KD diaphragm during aging. MHC-IIb was significantly decreased in aging wild type mouse diaphragm muscle, whereas aging ssTnT-KD diaphragm had an increase in MHC-IIb. *, $p < 0.05$ aging *versus* young groups of the same genotype; #, $p < 0.05$, ssTnT-KD *versus* wild type in the aging group, analyzed by two-tailed Student's *t* tests. *mN*, millinewtons.

ratio of myofilament proteins formed a basis of the fast-ward change of fiber types.

Because the diaphragm is a mixed fiber muscle (13), the decreases in the slow isoform myofilament proteins could reflect decreases in the number and/or size of slow fibers as well as increases in the number and/or size of fast fibers as a compensation for the decreases in ssTnT. Our results first showed reductions of both number and size of type 1 slow muscle fibers, which would directly contribute to the atrophy of ssTnT-KD mouse diaphragm. Although the number of type 2 fibers increased to compensate for the decreased number type 1 fibers, the cross-sectional area of type 2 fibers in ssTnT-KD diaphragm was decreased (Fig. 5*B*). Therefore, the atrophy of type 2 fibers that are the major fiber type in mouse diaphragm muscle (Fig. 5*A*) further contributed to the atrophy of ssTnT-KD diaphragm muscle. The mechanism for ssTnT deficiency to cause atrophy of fast type 2 fibers in diaphragm muscle remains to be investigated.

The effects of slow TnT deficiency on diaphragm myofilament protein contents exhibited aging related changes. Although both wild type and ssTnT-KD diaphragm muscles turned toward a slower fiber type in aging (Fig. 9), an interesting adaptation to ssTnT-KD was that MHC-IIb was significantly decreased in wild type but increased in ssTnT-KD diaphragm muscle. This adaptive sustainment of MHC-IIb that produces the fastest *in vitro* motility among MHC isoforms (26) may have contributed to the less slow-ward shift of the aging ssTnT-KD diaphragm muscle (Fig. 9*A*).

The finding that decreased expression of slow TnT resulted in a series of decreases in slow TnI and MHC-I indicated a consequence of fiber type switching. The finding that a change in one thin filament protein in skeletal muscle would cause multiple secondary changes in gene regulation suggests an experimental model to investigate the highly plastic nature of skeletal muscle during physiological and pathological adaptations.

Slow TnT Deficiency Reduces Fatigue Tolerance of Diaphragm Muscle—It has been established that stimulating skeletal muscle contraction with an electrical pulse of short duration (0.1–0.2 ms) significantly depends on the propagation of action potential along the plasma membrane (18). In contrast, electrical pulses with longer duration of 2.0 ms can propagate directly to the transverse tubular membranes, in which a majority of the L-type calcium channels are present, to activate calcium mobilization mechanisms with less dependence on plasma membrane action potential propagation, thus bypassing the fatigue mechanism of plasma membrane inexcitability (27). Therefore, we applied a high frequency fatigue stimulation protocol to dissect plasma membrane electrical fatigability and myofibril fatigability. The results clearly demonstrated that ssTnT deficiency significantly increased myofilament fatigability with unchanged plasma membrane excitability.

The increased myofilament fatigability of the ssTnT-KD mouse diaphragm muscle was further demonstrated using an intermittent tetanic fatigue protocol mimicking the respiratory contractions. The results confirmed the physiological impor-

tance of ssTnT in diaphragm function. The fatigability of ssTnT-KD diaphragm muscle shown by normalized force production (Fig. 8) demonstrated that in addition to the overall muscle atrophy, the qualitative changes of decreased number of slow fibers and slow isoforms of myofilament proteins severely impaired the fatigue tolerance of diaphragm muscle. In addition to explaining the terminal respiratory failure seen in virtually all Amish nemaline myopathy patients, the cTnI-KO/cTnI-ND double transgenic mouse model provides a highly valuable experimental system to study the pathogenesis, pathophysiology, and treatment of this devastating and lethal genetic disease.

Acknowledgments—We thank Hui Wang for PCR genotyping of transgenic mice, Dr. Xupei Huang (Florida Atlantic University) for providing the cTnI-KO mouse line, Dr. Jim Lin (University of Iowa) for providing the T12 mAb, and Dr. Jeffrey Robbins (University of Cincinnati) for the mouse cardiac α-MHC gene promoter used in the construction of cTnI-ND transgenic mouse lines.

REFERENCES

1. Perry, S. V. (1998) *J. Muscle Res. Cell Motil.* **19,** 575–602
2. Jin, J. P., Zhang, Z., and Bautista, J. A. (2008) *Crit. Rev. Eukaryot. Gene Expr.* **18,** 93–124
3. Johnston, J. J., Kelley, R. I., Crawford, T. O., Morton, D. H., Agarwala, R., Koch, T., Schäffer, A. A., Francomano, C. A., and Biesecker, L. G. (2000) *Am. J. Hum. Genet.* **67,** 814–821
4. Wang, X., Huang, Q. Q., Breckenridge, M. T., Chen, A., Crawford, T. O., Morton, D. H., and Jin, J. P. (2005) *J. Biol. Chem.* **280,** 13241–13249
5. Jin, J. P., Brotto, M. A., Hossain, M. M., Huang, Q. Q., Brotto, L. S., Nosek, T. M., Morton, D. H., and Crawford, T. O. (2003) *J. Biol. Chem.* **278,** 26159–26165
6. Huang, Q. Q., and Jin, J. P. (1999) *J. Mol. Evol.* **49,** 780–788
7. Huang, X., Pi, Y., Lee, K. J., Henkel, A. S., Gregg, R. G., Powers, P. A., and Walker, J. W. (1999) *Circ. Res.* **84,** 1–8
8. Jin, J. P. (1996) *Biochem. Biophys. Res. Commun.* **225,** 883–889
9. Barbato, J. C., Huang, Q. Q., Hossain, M. M., Bond, M., and Jin, J. P. (2005) *J. Biol. Chem.* **280,** 6602–6609
10. Yu, Z. B., Zhang, L. F., and Jin, J. P. (2001) *J. Biol. Chem.* **276,** 15753–15760
11. Subramaniam, A., Gulick, J., Neumann, J., Knotts, S., and Robbins, J. (1993) *J. Biol. Chem.* **268,** 4331–4336
12. Feng, H. Z., Hossain, M. M., Huang, X., and Jin, J. P. (2009) *Arch. Biochem. Biophys.* **487,** 36–41
13. Brotto, M. A., Biesiadecki, B. J., Brotto, L. S., Nosek, T. M., and Jin, J. P. (2006) *Am. J. Physiol. Cell Physiol* **290,** C567–C576
14. Jin, J. P., Chen, A., and Huang, Q. Q. (1998) *Gene* **214,** 121–129
15. Lin, J. J. (1981) *Proc. Natl. Acad. Sci. U.S.A.* **78,** 2335–2339
16. Feng, H. Z., Biesiadecki, B. J., Yu, Z. B., Hossain, M. M., and Jin, J. P. (2008) *J. Physiol.* **586,** 3537–3550
17. Feng, H. Z., Chen, M., Weinstein, L. S., and Jin, J. P. (2008) *J. Biol. Chem.* **283,** 33384–33393
18. Cairns, S. P., Chin, E. R., and Renaud, J. M. (2007) *J. Appl. Physiol* **103,** 359–368
19. Yu, Z. B., Gao, F., Feng, H. Z., and Jin, J. P. (2007) *Am. J. Physiol. Cell Physiol.* **292,** C1192–C1203
20. van Lunteren, E., and Moyer, M. (2003) *Respiration* **70,** 636–642
21. Larsson, L., Grimby, G., and Karlsson, J. (1979) *J. Appl. Physiol.* **46,** 451–456
22. Gannon, J., Doran, P., Kirwan, A., and Ohlendieck, K. (2009) *Eur J. Cell Biol.* **88,** 685–700
23. Gomes, A. V., Barnes, J. A., Harada, K., and Potter, J. D. (2004) *Mol. Cell. Biochem.* **263,** 115–129
24. Reiser, P. J., Westfall, M. V., Schiaffino, S., and Solaro, R. J. (1994) *Am. J. Physiol.* **267,** H1589–H1596
25. Chong, S. M., and Jin, J. P. (2009) *J. Mol. Evol.* **68,** 448–460
26. Degens, H., and Larsson, L. (2007) *J. Musculoskelet. Neuronal Interact.* **7,** 56–61
27. Cairns, S. P., Taberner, A. J., and Loiselle, D. S. (2009) *J. Appl. Physiol.* **106,** 101–112